

Neutralino Dark Matter and Other LHC Predictions from Quasi Yukawa Unification

Qaisar Shafi^{a1}, Şükrü Hanif Tanyıldızı^{b2} and Cem Salih Ün^{c3}

^a *Bartol Research Institute, Department of Physics and Astronomy,
University of Delaware, Newark, DE 19716, USA*

^b *Bogoliubov Laboratory of Theoretical Physics, Joint Institute for Nuclear Research,
141980, Dubna, Moscow Region, Russia*

^c *Department of Physics, Uludağ University, Bursa, Turkey, TR16059*

Abstract

We explore the dark matter and LHC implications of $t - b - \tau$ quasi Yukawa unification in the framework of supersymmetric models based on the gauge symmetry $G = SU(4)_c \times SU(2)_L \times SU(2)_R$. The deviation from exact Yukawa unification is quantified by a dimensionless parameter C ($|C| \lesssim 0.2$), such that the Yukawa couplings at M_{GUT} are related by $y_t : y_b : y_\tau = |1+C| : |1-C| : |1+3C|$. In contrast to earlier studies which focused on universal gaugino masses, we consider non-universal gaugino masses at M_{GUT} that are compatible with the gauge symmetry G . We perform two independent scans of the fundamental parameter space, one of which employs ISAJET, while the other uses SoftSusy interfaced with SuperIso. These scans reveal qualitatively similar allowed regions in the parameter space, and yield a variety of neutralino dark matter scenarios consistent with the observations. These include stau and chargino coannihilation scenarios, the A -resonance scenario, as well as Higgsino dark matter solution which is more readily probed by direct detection searches. The gluino mass is found to be $\lesssim 4.2$ TeV, the stop mass is $\gtrsim 2$ TeV, while the first two family squarks and sleptons are of order 4 – 5 TeV and 3 TeV respectively.

¹Email: shafi@bartol.udel.edu

²Email: hanif@theor.jinr.ru

³Email: cemsalihun@uludag.edu.tr

1 Introduction

In an earlier paper [1], hereafter referred to as I, we have explored the LHC implications of imposing $t - b - \tau$ Quasi-Yukawa Unification (QYU) at the grand unification scale ($M_{\text{GUT}} \sim 2 \times 10^{16}$ GeV). This modified approach to the third family ($t - b - \tau$) YU [2] can be motivated by the desire to construct realistic supersymmetric models of grand unified theories (GUTs) which also incorporate realistic masses and mixings observed in the matter sector. For instance, the desired quarks and charged lepton masses for the second family fermion can be incorporated, following [3], by including Higgs fields in the (15,1,3) representation of $G = SU(4)_c \times SU(2)_L \times SU(2)_R$ (4-2-2) [4], which develop a non-zero GUT scale vacuum expectation values (VEVs). The third family Yukawa couplings receive, in this case, sizable new contributions, and the deviations from exact YU can be stated as follows [1]:

$$y_t : y_b : y_\tau = |1 + C| : |1 - C| : |1 + 3C| \quad (1)$$

where C measures the deviation from the exact YU. Restricting the deviation to $C \lesssim 0.2$ we refer Eq.(1) to QYU condition.

The 4-2-2 model has many salient features distinguishing it from other high scale theories [5]. The discrete left-right (LR) symmetry reduces the number of gauge couplings from three to two with $g_L = g_R$. It also requires gaugino masses of $SU(2)_L$ and $SU(2)_R$ to be equal at M_{GUT} . The matter fields of each family belong to $\psi(4, 2, 1)$ and $\psi_c(\bar{4}, 1, 2)$. The LR symmetry requires the existence of right handed neutrino.

In this paper we reconsider QYU in the framework of 4-2-2 defined above, taking into account the fact that the MSSM gaugino masses $M_{1,2,3}$ at M_{GUT} can be non-universal. In particular, we assume the following asymptotic relation [6]

$$M_1 = \frac{3}{5}M_2 + \frac{2}{5}M_3 \quad , \quad (2)$$

which follows from the assumption of left-right symmetry at M_{GUT} and the fact that $U(1)_Y$ derived from 4-2-2 is given as follows;

$$Y = \sqrt{\frac{3}{5}}I_{3R} + \sqrt{\frac{2}{5}}(B - L). \quad (3)$$

Here M_1 , M_2 and M_3 are the asymptotic gaugino masses for $U(1)_Y$, $SU(2)_L$ and $SU(3)_c$, and I_{3R} and $(B - L)$ are diagonal generators of $SU(2)_R$ and $SU(4)_c$ respectively.

The setup of our paper is as follows. In Section 2 we briefly explain our scanning procedure and list the experimental constraints that we impose on the data obtained from our scans. In Section 3 we show the fundamental parameter space that is allowed by the experimental constraints and QYU. Section 4 provides the implications for dark

matter sector such as coannihilation channels and the resonance solution. Section 5 considers a Higgsino-like LSP and emphasize the implications for direct detection experiments. Section 6 compares the ISAJET and SoftSusy, and the small variations in their phenomenology. We also present the benchmark points obtained from the different scans to exemplify our results. Finally, we conclude our study in Section 7.

2 Scanning Procedure and Experimental Constraints

In our scan, we employ ISAJET 7.84 [7], SoftSusy-3.4.1 [8] and SuperIso Relic v3.3 [9] to calculate the low scale observables. The gauge and Yukawa couplings are first estimated at the low scale. ISAJET evolves the gauge couplings and the Yukawa couplings of the third family up to M_{GUT} , while SoftSusy performs the calculations in the three family approximation in evolution of Yukawa couplings. We do not strictly enforce the gauge unification condition $g_1 = g_2 = g_3$, since a few percent deviation from the gauge coupling unification can be generated by unknown GUT-scale threshold corrections [10]. Hence, M_{GUT} is calculated to be the scale where $g_1 = g_2$ and g_3 deviates a few percent. After M_{GUT} is determined, the soft supersymmetry breaking (SSB) parameters determined with the boundary conditions defined at M_{GUT} are evolved together with the gauge and Yukawa couplings from M_{GUT} to the weak scale M_Z .

The SUSY threshold corrections to the Yukawa couplings [11] are taken into account at the common scale $M_{\text{SUSY}} = \sqrt{m_{\tilde{t}_L} m_{\tilde{t}_R}}$ in ISAJET, while SoftSusy evaluates them at the electroweak scale. The entire parameter set is iteratively run between M_Z and M_{GUT} using full 2-loop RGEs, and the SSB parameters are extracted from RGEs at the appropriate scales $m_i = m_i(m_i)$.

We have performed random scans over the following parameter space:

$$\begin{aligned}
0 &\leq m_{16} \leq 10000 \text{ GeV} \\
0 &\leq M_2 \leq 2000 \text{ GeV} \\
0 &\leq M_3 \leq 2000 \text{ GeV} \\
-3 &\leq A_0/m_{16} \leq 3 \\
40 &\leq \tan \beta \leq 60 \\
0 &\leq m_{10} \leq 10000 \text{ GeV} \\
\mu &> 0, \quad m_t = 173.3 \text{ GeV},
\end{aligned} \tag{4}$$

taking Eq.2 into account. We use the $SO(10)$ notation in which m_{16} is the universal SSB mass term for the particles, and M_1, M_2, M_3 are SSB mass terms for the gauginos

of $U(1)_Y$, $SU(2)_L$ and $SU(3)_c$ respectively, A_0 is the universal SSB term for trilinear scalar interactions, $\tan\beta$ is the ratio of VEVs of the MSSM higgs doublets, μ is coefficient of the bilinear Higgs mixing term, and m_t is the top quark mass. Note that we set the top quark mass to 173.3 GeV [12, 13], and our results are not too sensitive to a $1\sigma - 2\sigma$ variation in m_t [14].

We employ the Metropolis-Hasting algorithm as described in [15], and require all collected points to satisfy radiative electroweak symmetry breaking (REWSB) with LSP neutralino. The REWSB gives a crucial theoretical constraint on the parameter space [16]. After collecting data, we impose constraints from the mass bounds [17], rare decays of B-meson such as $B_s \rightarrow \mu^+\mu^-$ [18], $b \rightarrow s\gamma$ [19], and $B_u \rightarrow \tau\nu_\tau$ [20]. After obtaining the region allowed by the LHC constraints, we also apply the WMAP bound [21] on the relic abundance of LSP neutralino. ISAJET interfaces with IsaTools [22, 23] for B-physics and relic density observables, while we interface SoftSusy with SuperIso Relic in order to calculate these observables. The experimental constraints imposed in our data can be summarized as follows:

$$\begin{aligned}
m_h &= (123 - 127) \text{ GeV} \\
m_{\tilde{g}} &\leq 1 \text{ TeV} \\
0.8 \times 10^{-9} &\leq \text{BR}(B_s \rightarrow \mu^+\mu^-) \leq 6.2 \times 10^{-9} \text{ (} 2\sigma \text{)} \\
2.99 \times 10^{-4} &\leq \text{BR}(b \rightarrow s\gamma) \leq 3.87 \times 10^{-4} \text{ (} 2\sigma \text{)} \\
0.15 &\leq \frac{\text{BR}(B_u \rightarrow \tau\nu_\tau)_{\text{MSSM}}}{\text{BR}(B_u \rightarrow \tau\nu_\tau)_{\text{SM}}} \leq 2.41 \text{ (} 3\sigma \text{)} \\
0.0913 &\leq \Omega_{\text{CDM}} h^2 \leq 0.1363 \text{ (} 5\sigma \text{)}.
\end{aligned} \tag{5}$$

We emphasize here the mass bounds on the Higgs boson [24, 25] and gluino [26]. We allow a few percent deviation from the observed mass of the Higgs boson, since there exist about a 2 GeV error in estimation of its mass arising due to theoretical uncertainties in the calculation of the minimum of the scalar potential, and experimental uncertainties in m_t and α_s [27]. Besides these constraints, we require our solutions to do no worse than the SM in comparing predictions for the muon anomalous magnetic moment. Note that we relax the WMAP bound to $0.0913 \leq \Omega_{\text{CDM}} h^2 \leq 1$ on the solutions obtained from SuperIso Relic in order to take into account uncertainties in the calculation of the relic abundance of LSP neutralino.

3 Fundamental Parameter Space of Quasi Yukawa Unification and Sparticle Mass Spectrum

In this section, we highlight the allowed regions in the fundamental parameter space of 4-2-2 given in Eq.(4) and present the results for the supersymmetric particles and

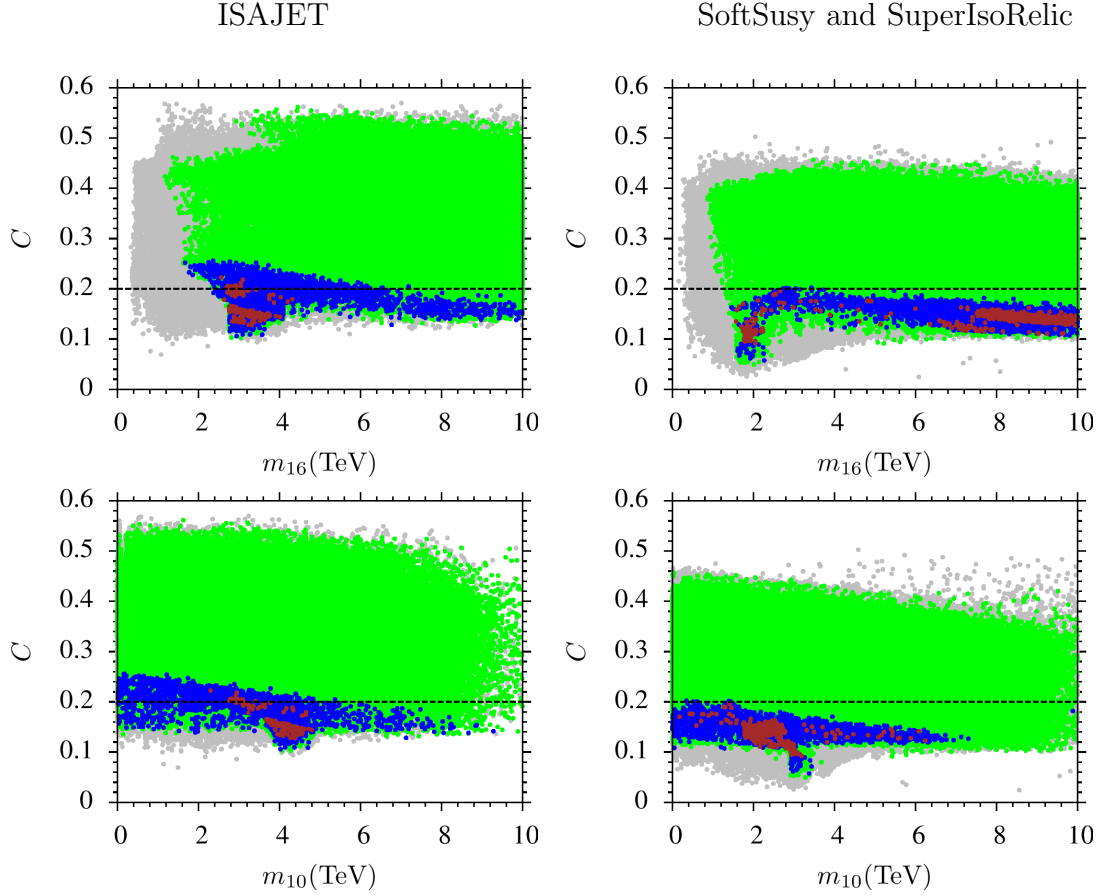


Figure 1: Plots in $C - m_{16}$ and $C - m_{10}$ planes. The left panel shows the results obtained by using ISAJET, while the right panels display the results from SoftSusy. All points are compatible with REWSB and LSP neutralino. Green points satisfy the mass bounds on the sparticles and the constraints from rare B-decays. Blue points form a subset of green and they are compatible with the QYU condition. Points in red form a subset of blue and satisfy the constraint on relic abundance of LSP neutralino. They are consistent with the WMAP bound within 5σ uncertainty in ISAJET plots, while $0.0913 \leq \Omega h^2 \leq 1$ for those obtained from SoftSusy and SuperIso Relic.

Higgs boson mass spectrum that we obtain from the scans using ISAJET and SoftSusy which is interfaced with SuperIso Relic. Fig. 1 shows the plots in $C - m_{16}$ and $C - m_{10}$ planes. The left panel shows the results obtained by using ISAJET, while the right panels displays the results from SoftSusy. All points are compatible with REWSB and LSP neutralino. Green points satisfy the mass bounds on the sparticles and

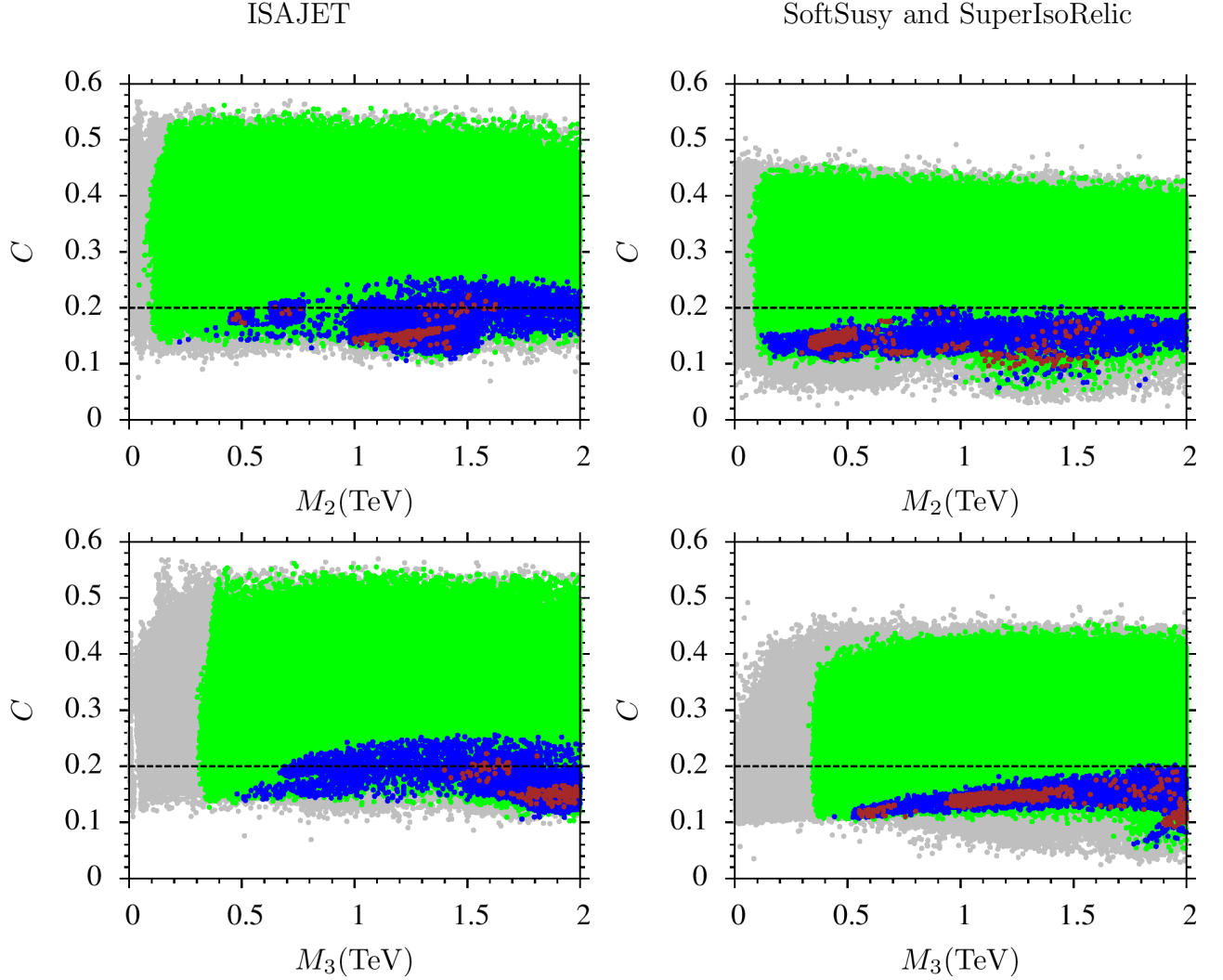


Figure 2: Plots in $C - M_2$ and $C - M_3$ planes. Color coding is the same as in Fig.1.

the constraints from rare B-decays. Blue points form a subset of green and they are compatible with the QYU condition. Points in red are a subset of blue, and satisfy the constraint on relic abundance of LSP neutralino. They are consistent with the WMAP bound within 5σ uncertainty in ISAJET plots, while $0.0913 \leq \Omega h^2 \leq 1$ for those obtained from SoftSusy and SuperIso Relic. As seen from the $C - m_{16}$ panels, QYU (blue) requires $m_{16} \gtrsim 2$ TeV, while m_{10} is only loosely constrained.

Similarly Fig.2 displays the plots in $C - M_2$ and $C - M_3$ planes. Color coding is the same as in Fig.1. We can see from the $C - M_2$ panel that M_2 can be as low

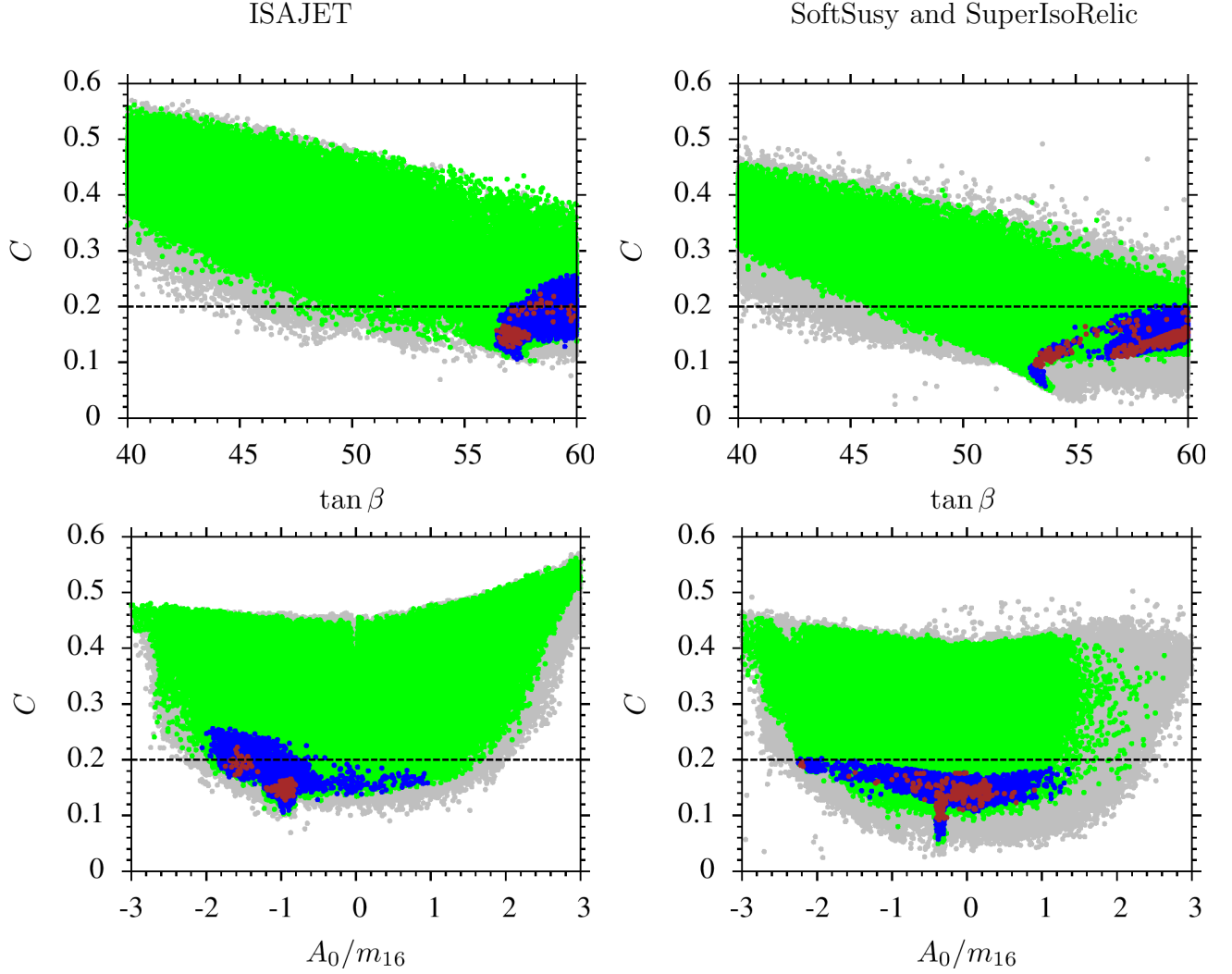


Figure 3: Plots in $C - \tan \beta$ and $C - A_0/m_{16}$ planes. Color coding is the same as in Fig.1.

as 300 GeV. Such light M_2 solutions yield bino-wino mixing at the low scale which plays a role in reducing the relic abundance of LSP neutralino to the desired range. The $C - M_3$ plane shows that $M_3 \gtrsim 500$ GeV is compatible with QYU which leads to a heavy gluino ($m_{\tilde{g}} \gtrsim 1.5$ TeV) at low scale.

The results for the remaining parameters are shown in Fig.3 with plots in $C - \tan \beta$ and $C - A_0/m_{16}$ planes. Color coding is the same as in Fig.1. The plots in the $C - \tan \beta$ planes shows that QYU requires rather high $\tan \beta$ values. The top left

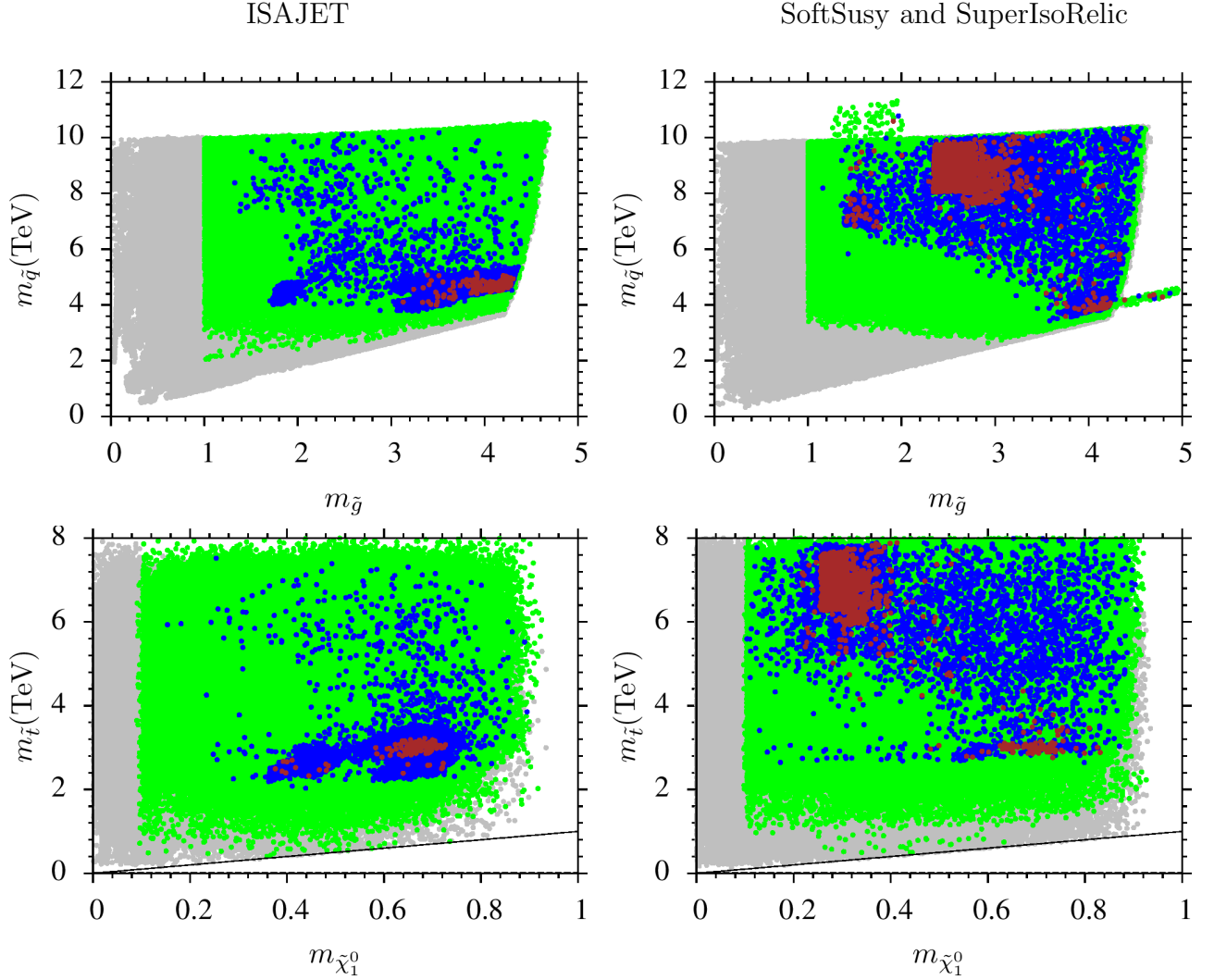


Figure 4: Plots in $C - m_{\tilde{g}}$ and $C - m_{\tilde{t}}$ planes. Color coding is the same as in Fig.1. The blue points satisfy $C \leq 0.2$ as well as QYU condition.

panel shows that $\tan\beta \gtrsim 56$ is compatible with QYU, while it is possible to find QYU solutions with SoftSusy for $\tan\beta \gtrsim 53$. The $C - A_0/m_{16}$ panels from both ISAJET and SoftSusy show that A_0/m_{16} can lie in the range $(-2, 1)$.

We present the results for the mass spectrum of the colored particles in Fig.4 in $C - m_{\tilde{g}}$ and $C - m_{\tilde{t}}$ planes. Color coding is the same as in Fig.1. In addition, the blue points satisfy $C \leq 0.2$ as well as QYU condition. The gluino mass compatible with QYU and $C \leq 0.2$ is found to be $m_{\tilde{g}} \gtrsim 1.5$ TeV as stated above, and it can be

tested in future experiments at the Large Hadron Collider (LHC). Similarly, the stop quarks satisfy $m_{\tilde{t}} \gtrsim 2$ TeV. ISAJET and SoftSusy are in good agreement regarding results of the mass spectrum.

4 LSP Neutralino and Coannihilation Scenarios

In the previous section we have focused on the fundamental parameter space and the mass spectrum of the colored particles. Since we accept only those solutions which lead to LSP neutralino, it is worth investigating the implications of 4-2-2 on the dark matter observables. Indeed, if the LSP neutralino is mostly a bino, its relic abundance is usually so high that it cannot be consistent with the WMAP observation. However, one can identify various coannihilation channels that reduce the relic abundance of neutralino to the desired ranges. 4-2-2 has some rich phenomenological implications and allows various coannihilation channel scenarios at the low scale [28], since it allows asymptotically different masses for the gauginos as given in Eq.(2). On the other hand, if one imposes $t - b - \tau$ YU at M_{GUT} with $\mu > 0$, only the gluino-neutralino coannihilation channel can survive [6]. Relaxing this to $b - \tau$ YU opens up, in addition, the stop-neutralino channel [29]. In this section, we consider the phenomenological implications of QYU in 4-2-2 regarding the dark matter and the structure of LSP neutralino. Besides the bino-like LSP neutralino, it is possible to find solutions with bino-wino mixture, bino-higgsino mixture, or mostly higgsino LSP neutralino which leads to different phenomenology.

Fig.5 displays the results in $M_2 - M_1$ and $\mu - M_1$ planes. Color coding is the same as in Fig.4. As stated in the previous section, M_2 can be as low as 300 GeV. The line in $M_2 - M_1$ plane indicates solutions for which $M_1 = 2M_2$ and they yield bino-wino mixing at the low scale. Similarly, the line in $\mu - M_1$ plane corresponds to the solutions which have $M_1 = \mu$. These solutions can lead to very interesting implications, since LSP neutralino is bino-higgsino mixture near this line. Moreover, the LSP neutralino is found to be mostly higgsino below the line.

Fig.6 summarizes our results for the coannihilation channels compatible with QYU in $m_{\tilde{\chi}_1^\pm} - m_{\tilde{\chi}_1^0}$, $m_{\tilde{\tau}} - m_{\tilde{\chi}_1^0}$, and $m_A - m_{\tilde{\chi}_1^0}$ planes. Color coding is the same as in Fig.4. The solid lines in the plots correspond to the related coannihilation channel regions. The ISAJET panel of $m_{\tilde{\chi}_1^\pm} - m_{\tilde{\chi}_1^0}$ shows that the neutralino and the lightest chargino of mass $\gtrsim 400$ GeV can be nearly degenerate as expected from the $M_2 - M_1$ planes of Fig.5. We can find solutions with chargino-neutralino coannihilation channel for $m_{\tilde{\chi}_1^\pm} \simeq m_{\tilde{\chi}_1^0} \sim 200$ GeV, if we relax the LSP neutralino relic density to $0.0913 \leq \Omega h^2 \leq 1$, as seen in the SoftSusy and SuperIso Relic panel. Besides chargino-neutralino coannihilation, the stau-neutralino channel is found to be compatible with QYU as seen from the $m_{\tilde{\tau}} - m_{\tilde{\chi}_1^0}$ plane. There are plenty of solutions for $400 \lesssim m_{\tilde{\tau}} \simeq m_{\tilde{\chi}_1^0} \lesssim 800$ GeV in the ISAJET panel, while SoftSusy yields fewer solutions with light

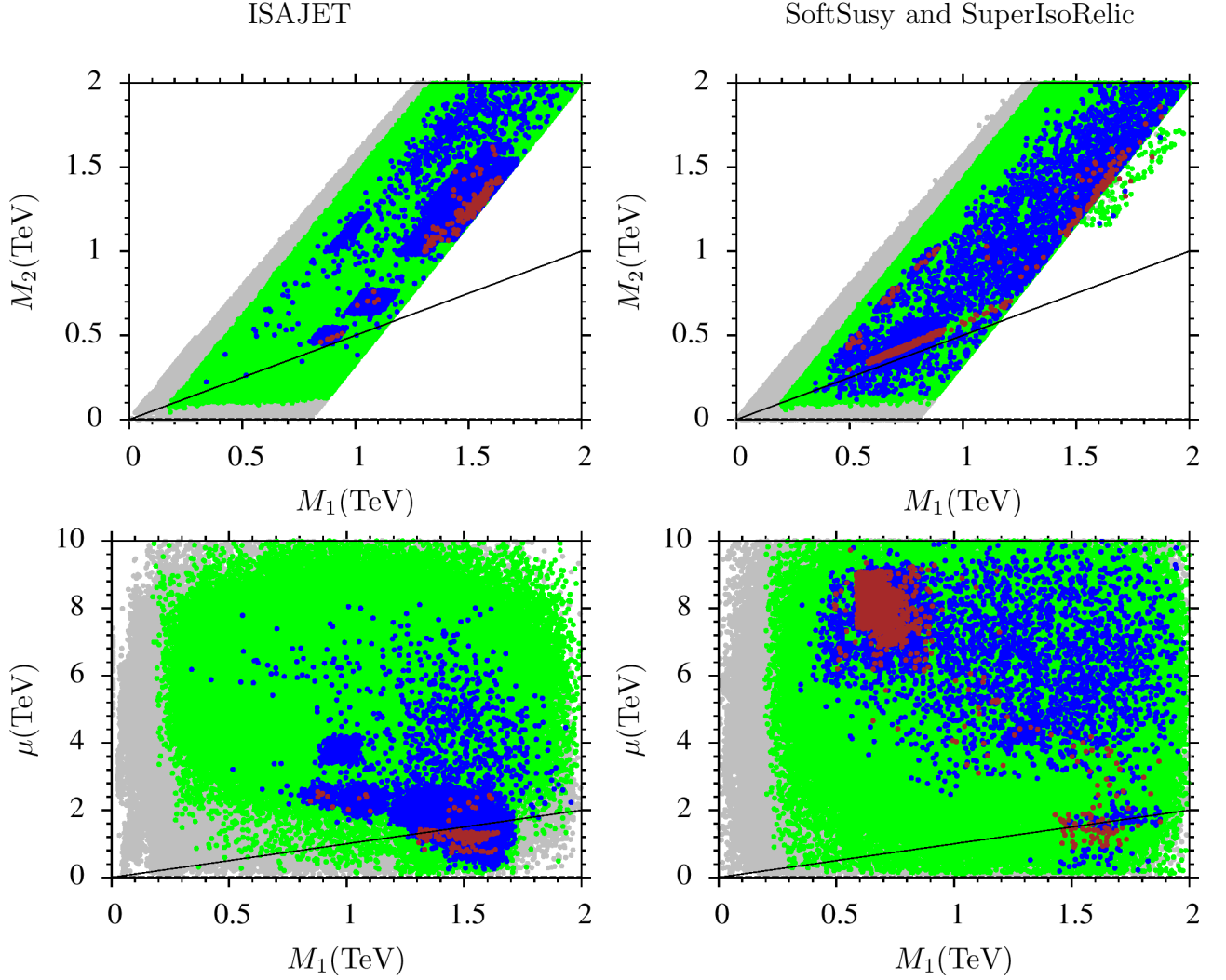


Figure 5: Plots in $M_2 - M_1$ and $\mu - M_1$ planes. Color coding is the same as Fig.4.

staus.

Another solution allowed by QYU is the A -resonance shown in the $m_A - m_{\tilde{\chi}_1^0}$ planes. The solid line in these panels corresponds to $m_A = 2m_{\tilde{\chi}_1^0}$ in which two LSP neutralinos annihilate via the A -boson. The A -resonance solutions can be found for $m_{\tilde{\chi}_1^0} \gtrsim 600$ GeV in the data set obtained from ISAJET, while it can be realized for $m_{\tilde{\chi}_1^0} \gtrsim 600$ if one applies $0.0913 \leq \Omega h^2 \leq 1$ to the data set obtained with SoftSusy and SuperIso.

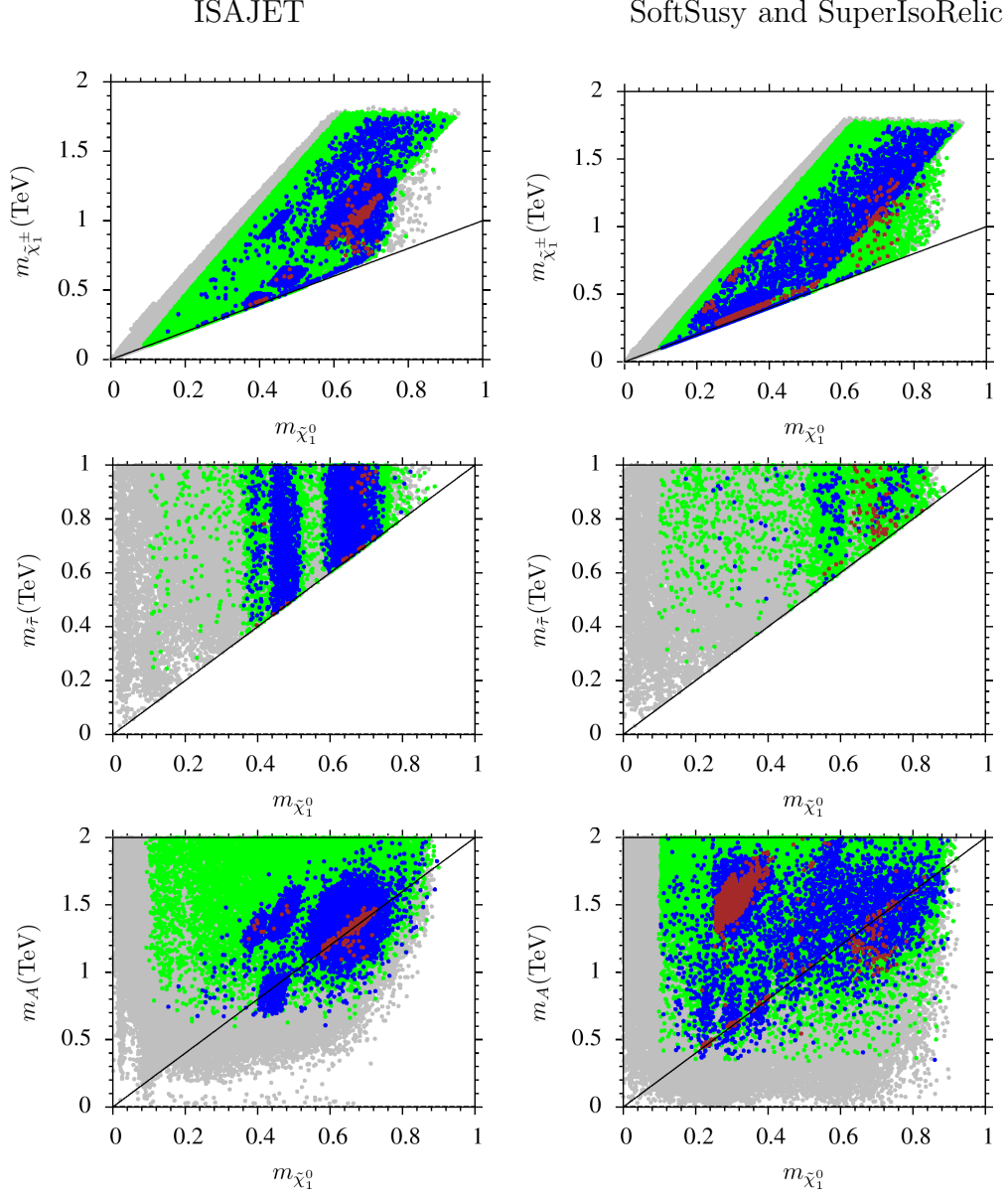


Figure 6: Plots in $m_{\tilde{\chi}_1^\pm} - m_{\tilde{\chi}_1^0}$, $m_{\tilde{\tau}} - m_{\tilde{\chi}_1^0}$, and $m_A - m_{\tilde{\chi}_1^0}$ planes. Color coding is the same as in Fig.4. The solid lines in the plots correspond to the related coannihilation channel regions.

5 Higgsino(-like) LSP

In the previous section we have identified various coannihilation channels and a resonance solution which reduce the relic abundance of LSP neutralino so that the dark

matter phenomenology in the 4-2-2 framework can be consistent with the WMAP experiment. In this section we briefly explore an alternative scenario in which the LSP neutralino is a gaugino-higgsino. This case opens up possibilities for direct detection experiments via relic LSP neutralino scattering on nuclei. The case with bino-wino mixture, or equivalently those with chargino-neutralino coannihilation, yield moderate cross-sections in these scattering processes, since the LSP interacts with quarks in the nucleon also via $SU(2)$ interactions. The scattering cross-section reaches its highest values when the LSP neutralino is a bino-higgsino mixture or mostly higgsino, since the Yukawa interactions between quarks and the higgsino component of LSP neutralino take part in the scattering processes.

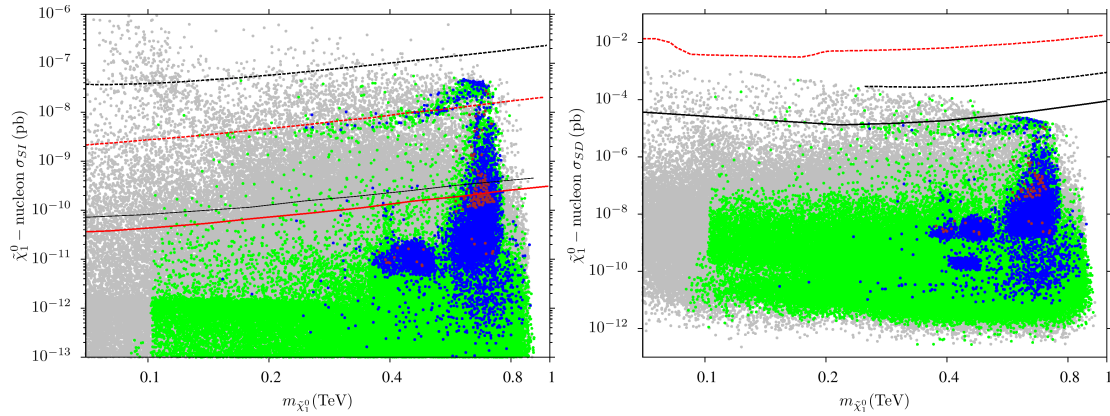


Figure 7: Plots in $\tilde{\chi}_1^0$ – nucleon σ_{SI} and $\tilde{\chi}_1^0$ – nucleon σ_{SD} planes. Color coding is the same as in Fig.4. In $\tilde{\chi}_1^0$ – nucleon σ_{SI} plane the dashed (solid) red line represents the current (future) bound of the XENON1T experiment, while the dashed (solid) black line show the current (future) bound of the CDMS experiment. In $\tilde{\chi}_1^0$ – nucleon σ_{SD} plane the dashed red line represents the bound from the Super K experiment, while the dashed (solid) black line shows the current (future) reach of the IceCube experiment.

We present our results in Fig.7 for neutralino-nucleon scattering for both spin-independent and spin-dependent cases in $\tilde{\chi}_1^0$ – nucleon σ_{SI} and $\tilde{\chi}_1^0$ – nucleon σ_{SD} planes. Color coding is the same as in Fig.4. In the $\tilde{\chi}_1^0$ – nucleon σ_{SI} plane, the dashed (solid) red line represents the current (future) bound of the XENON1T experiment, while the dashed (solid) black line shows the current (future) bound of the CDMS experiment. In the $\tilde{\chi}_1^0$ – nucleon σ_{SD} plane, the dashed red line represents the bound from the Super K experiment, while the dashed (solid) black line shows the current (future) reach of the IceCube experiment. Only the results from ISAJET are shown in the panels. As seen from the $\tilde{\chi}_1^0$ – nucleon σ_{SI} and $\tilde{\chi}_1^0$ – nucleon σ_{SD} plane, the spin-independent cross-section for the LSP neutralino with bino-wino mixture is

of order 10^{-11} pb, while it rises by two orders of magnitude for bino-higgsino mixture. Furthermore, the spin-independent cross-section lies between $10^{-10} - 10^{-8}$ pb if the LSP neutralino is mostly a higgsino within reach of the direct detection experiments such as XENON1T and SuperCDMS. Finally, we also check that QYU with Higgsino(-like) dark matter and mass ~ 1 TeV is also realized in 4-2-2 and $SO(10)$ supersymmetric models with universal gaugino masses (namely CMSSM boundary conditions) at M_{GUT} .

6 Comparison of ISAJET and SoftSusy

Ref. [30] gives a detailed analysis and comparison among several numerical codes including ISAJET and SoftSusy. In Sec.3 we show that QYU prefers regions with larger $\tan\beta$, and a 3% difference between the Yukawa couplings obtained from SoftSusy and ISAJET [30] can lead to some quantitative differences in the results.

In this section, we present two tables of benchmark points that exemplify the results obtained from our scans. Table 1 presents four benchmark points obtained from the ISAJET scan. The points are chosen to be consistent with the constraints mentioned in Sec.2. Point 1 is an A -resonance solution, and point 2 depicts a solution with higgsino dark matter. Points 3 and 4 display stau-neutralino and chargino-neutralino coannihilation solutions respectively. Point 4 also exemplifies the solution with the heaviest CP-even Higgs boson mass we obtained.

Similarly Table 2 displays four benchmark points consistent with the experimental constraints obtained from SoftSusy and SuperIso Relic scan. The points are chosen to be consistent with the constraints mentioned in Sec.2. Point 1 displays an A -resonance solution. Points 2 and 3 depict solutions with the higgsino dark matter, while WMAP bound on relic abundance of LSP neutralino is satisfied through the stau-neutralino coannihilation for Point 2, and chargino-neutralino coannihilation for Point 3. Point 4 also shows a solution with chargino-neutralino coannihilation and exemplifies the solution with the heaviest CP-even Higgs boson mass obtained.

Tables 1 and 2 also summarize the differences between ISAJET and SoftSusy in the fundamental parameters that yield similar implications. The gaugino masses differ a few hundred GeV in the case of stau-neutralino coannihilation, while it rises up to about 1 TeV in scalar masses m_{16} and m_{10} . The largest difference can be realized at the Point 4's which displays the largest SM-like Higgs boson mass from both scan. m_{16} is about 4 TeV heavier in SoftSusy result, while m_{10} is about 2 TeV lighter. On the other hand, the phenomenological results obtained from the scans yield very similar results. The fundamental parameter space allowed by the experimental results and QYU are quite similar, and the same coannihilation channels are identified from both scans.

ISAJET	Point 1	Point 2	Point 3	Point 4
m_0	3362	3312	2905	3844
M_1	1343	1615	1436	893
M_2	1143	1407	1365	480.3
M_3	1643	1929	1542	1512
m_{10}	4058	4377	3332	4320
$\tan \beta$	57.1	57.2	57.4	59.7
A_0/m_0	-1.05	-0.94	-1.46	-1.74
m_t	173.3	173.3	173.3	173.3
μ	1420	752	2477	1996
m_h	123.1	123.4	123.8	124.7
m_H	1205	1126	1330	1394
m_A	1197	1118	1322	1385
m_{H^\pm}	1209	1130	1334	1397
$m_{\tilde{\chi}_{1,2}^0}$	595.8, 958.5	701, 766	639, 1150	397.2, 413.9
$m_{\tilde{\chi}_{3,4}^0}$	959.3, 1343	773, 1189	2000, 2003	2474, 2475
$m_{\tilde{\chi}_{1,2}^\pm}$	959.3, 1343	775, 1168	1151, 2003	414.5, 2476
$m_{\tilde{g}}$	3628	4174	3399	3408
$m_{\tilde{u}_{L,R}}$	4533, 4507	4860, 4816	4118, 4061	4726, 4737
$m_{\tilde{t}_{1,2}}$	2772, 3251	3044, 3517	2388, 2947	2395, 3053
$m_{\tilde{d}_{L,R}}$	4534, 4501	4861, 4816	4119, 4054	4726, 4737
$m_{\tilde{b}_{1,2}}$	3223, 3457	3489, 3670	2915, 3117	3028, 3459
$m_{\tilde{\nu}_{e,\mu}}$	3441	3434	3036	3854
$m_{\tilde{\nu}_\tau}$	2662	2647	2264	2750
$m_{\tilde{e}_{L,R}}$	3441, 3395	3434, 3362	3037, 2951	3854, 3856
$m_{\tilde{\tau}_{1,2}}$	1398, 2659	1293, 2644	650.7, 2263	405.6, 2748
$\sigma_{SI}(\text{pb})$	0.13×10^{-9}	0.23×10^{-7}	0.26×10^{-10}	0.86×10^{-11}
$\sigma_{SD}(\text{pb})$	0.43×10^{-7}	0.94×10^{-5}	0.56×10^{-8}	0.27×10^{-8}
Ωh^2	0.108	0.104	0.128	0.106
$y_{t,b,\tau}(M_{\text{GUT}})$	0.56, 0.41, 0.70	0.56, 0.44, 0.70	0.55, 0.38, 0.72	0.54, 0.37, 0.70
C	0.15	0.13	0.18	0.18

Table 1: Benchmark points from ISAJET scan. The points are chosen to be consistent with the constraints mentioned in Sec.2. Point 1 is an A -resonance solution, Point 2 depicts a solution with the higgsino dark matter, the WMAP bound on relic abundance of LSP neutralino is satisfied through chargino-neutralino coannihilation for this point. Point 3 and Point 4 display stau-neutralino and chargino-neutralino coannihilation solutions respectively.

SoftSusy+ SuperIso Relic	Point 1	Point 2	Point 3	Point 4
m_0	1930	1820	2048	9832
M_1	1457	1649	1510	861.2
M_2	1096	1470	1218	479.4
M_3	1999	1918	1949	1434
m_{10}	2873	2972	3189	2130
$\tan \beta$	54.3	53.2	53.4	59.2
A_0/m_0	-0.41	-0.36	-0.37	-0.16
m_t	173.3	173.3	173.3	173.3
μ	1678	962.4	903.3	7593
m_h	123.2	123.1	123.3	125
m_H	1259	1000	948.2	1884
m_A	1259	1000	948.1	1884
m_{H^\pm}	1262	1004	952.2	1886
$m_{\tilde{\chi}_{1,2}^0}$	635.1 , 897.2	704 , 770	644.1 , 722	386.9 , 413.9
$m_{\tilde{\chi}_{3,4}^0}$	1348, 1354	778.4, 1219	723.8, 1014	7569, 7569
$m_{\tilde{\chi}_{1,2}^\pm}$	897.3, 1355	762, 1219	710.7 , 1014	413.7 , 7569
$m_{\tilde{g}}$	4220	4053	4129	3394
$m_{\tilde{u}_{L,R}}$	4086, 4056	3963, 3888	4082, 4041	10040, 10054
$m_{\tilde{t}_{1,2}}$	3066, 3302	2867, 3147	2965, 3211	7779, 8223
$m_{\tilde{d}_{L,R}}$	4087, 4048	3964, 3876	4084, 4033	10041, 10056
$m_{\tilde{b}_{1,2}}$	3272, 3377	3117, 3154	3185, 3259	8215, 8661
$m_{\tilde{\nu}_{e,\mu}}$	2054, 2053	2055, 2053	2192, 2191	9817, 9813
$m_{\tilde{\nu}_\tau}$	1621	1632	1734	8719
$m_{\tilde{e}_{L,R}}$	2056, 2003	2056, 1918	2194, 2121	9817, 9829
$m_{\tilde{\tau}_{1,2}}$	899.1, 1627	735.7 , 1635	937.3, 1737	7489, 8722
Ωh^2	0.103	0.13	0.095	0.092
$y_{t,b,\tau}(M_{\text{GUT}})$	0.56, 0.44, 0.67	0.56, 0.46, 0.66	0.56, 0.46, 0.65	0.54, 0.40, 0.67
C	0.12	0.10	0.09	0.15

Table 2: Benchmark points from SoftSusy and SuperIso Relic scan. The points are chosen to be consistent with the constraints mentioned in Sec.2. Point 1 displays an A -resonance solution. Points 2 and 3 depict solutions with the higgsino dark matter, while WMAP bound on relic abundance of LSP neutralino is satisfied through the stau-neutralino coannihilation for Point 2, and chargino-neutralino coannihilation for Point 3. Point 4 also shows a solution with chargino-neutralino coannihilation and exemplifies the solution with the heaviest CP-even Higgs boson mass obtained.

7 Conclusion

We have employed ISAJET and SoftSusy interfaced with SuperIso relic to explore the LHC implications of Quasi-Yukawa unified (QYU) supersymmetric models based on $G = SU(4)_c \times SU(2)_L \times SU(2)_R$. In these QYU models, the third family Yukawa unification relations involving t , b and τ , is quantified by a parameter C which takes values $\sim 0.1 - 0.2$. In contrast to earlier studies, the MSSM gaugino masses at M_{GUT} are non-universal but consistent with the gauge symmetry G . The thermal relic abundance of the LSP neutralino is compatible with the WMAP bounds through the chargino and stau coannihilation channels, as well as the A-resonance solution. We also identify solutions with Higgsino-like and pure Higgsino dark matter ($\mu \lesssim 1$ TeV) which can be tested in the direct dark matter searches such as XENON1T and SuperCDMS. The predicted gluino mass ranges from 1-4 TeV, while the stop masses are heavier than 2 TeV or so. It is reassuring to note that the low energy phenomenology obtained from ISAJET and SoftSusy are in good qualitative agreement.

Acknowledgment

We thank Ilia Gogoladze, M. Adeel Ajaib and Dimitri I. Kazakov for useful discussions. ŞHT would like to thank Michael Afanasev for his advice in programming. This work is supported in part by DOE Grants DE-FG02-91ER40626 (QS) and Russian Foundation for Basic Research (RFBR) Grant No. 14-02-00494-a (ŞHT). This work used the Extreme Science and Engineering Discovery Environment (XSEDE), which is supported by the National Science Foundation grant number OCI-1053575. Part of the numerical calculations reported in this paper were performed at the National Academic Network and Information Center (ULAKBIM) of Turkey Scientific and Technological Research Institution (TUBITAK), High Performance and Grid Computing Center (TRUBA Resources).

References

- [1] S. Dar, I. Gogoladze, Q. Shafi and C. S. Un, Phys. Rev. D **84**, 085015 (2011) [arXiv:1105.5122 [hep-ph]].
- [2] B. Ananthanarayan, G. Lazarides and Q. Shafi, Phys. Rev. D **44**, 1613 (1991; Phys. Lett. B **300**, 24 (1993)5; Q. Shafi and B. Ananthanarayan, Trieste HEP Cosmol.1991:233-244.
- [3] M. E. Gomez, G. Lazarides and C. Pallis, Nucl. Phys. B **638**, 165 (2002) [hep-ph/0203131]; M. E. Gomez, G. Lazarides and C. Pallis, Phys. Rev. D **67**, 097701 (2003) [hep-ph/0301064]; C. Pallis and M. E. Gomez, hep-ph/0303098;

- [4] J. C. Pati and A. Salam, Phys. Rev. D **10**, 275 (1974).
- [5] G. Lazarides and Q. Shafi, Nucl. Phys. B **189**, 393 (1981); S. F. King and Q. Shafi, Phys. Lett. B **422**, 135 (1998) [hep-ph/9711288]; G. Lazarides, M. Magg and Q. Shafi, Phys. Lett. B **97**, 87 (1980); T. W. Kephart, C. A. Lee and Q. Shafi, JHEP **0701**, 088 (2007) [hep-ph/0602055]; T. W. Kephart and Q. Shafi, Phys. Lett. B **520**, 313 (2001) [hep-ph/0105237]; R. N. Mohapatra and J. C. Pati, Phys. Rev. D **11**, 566 (1975); G. Senjanovic and R. N. Mohapatra, Phys. Rev. D **12**, 1502 (1975); G. Senjanovic, Nucl. Phys. B **153**, 334 (1979); M. Magg, Q. Shafi and C. Wetterich, Phys. Lett. B **87**, 227 (1979); M. Cvetič, Nucl. Phys. B **233**, 387 (1984); T. W. B. Kibble, G. Lazarides and Q. Shafi, Phys. Lett. B **113**, 237 (1982); Phys. Rev. D **26**, 435 (1982); R. N. Mohapatra and B. Sakita, Phys. Rev. D **21**, 1062 (1980).
- [6] I. Gogoladze, R. Khalid and Q. Shafi, Phys. Rev. D **79**, 115004 (2009) [arXiv:0903.5204 [hep-ph]].
- [7] F. E. Paige, S. D. Protopopescu, H. Baer and X. Tata, hep-ph/0312045; For updates and changes in the current version, see [ISAJET 7.84](#)
- [8] B. C. Allanach, Comput. Phys. Commun. **143**, 305 (2002) [hep-ph/0104145].
- [9] F. Mahmoudi, Comput. Phys. Commun. **180**, 1579 (2009) [arXiv:0808.3144 [hep-ph]]; F. Mahmoudi, Comput. Phys. Commun. **180**, 1718 (2009); A. Arbey and F. Mahmoudi, Comput. Phys. Commun. **181**, 1277 (2010) [arXiv:0906.0369 [hep-ph]].
- [10] J. Hisano, H. Murayama, and T. Yanagida, Nucl. Phys. **B402** (1993) 46; Y. Yamada, Z. Phys. **C60** (1993) 83; J. L. Chkareuli and I. G. Gogoladze, Phys. Rev. D **58**, 055011 (1998).
- [11] D. M. Pierce, J. A. Bagger, K. T. Matchev and R. j. Zhang, Nucl. Phys. B **491**, 3 (1997) [hep-ph/9606211].
- [12] [ATLAS and CDF and CMS and D0 Collaborations], arXiv:1403.4427 [hep-ex].
- [13] I. Gogoladze, R. Khalid, S. Raza and Q. Shafi, arXiv:1402.2924 [hep-ph].
- [14] I. Gogoladze, R. Khalid, S. Raza and Q. Shafi, JHEP **1106** (2011) 117.
- [15] G. Belanger, F. Boudjema, A. Pukhov and R. K. Singh, JHEP **0911**, 026 (2009); H. Baer, S. Kraml, S. Sekmen and H. Summy, JHEP **0803**, 056 (2008).

- [16] L. E. Ibanez and G. G. Ross, *Phys. Lett.* **B110** (1982) 215; K. Inoue, A. Kakuto, H. Komatsu and S. Takeshita, *Prog. Theor. Phys.* **68**, 927 (1982) [Erratum-ibid. **70**, 330 (1983)]; L. E. Ibanez, *Phys. Lett.* **B118** (1982) 73; J. R. Ellis, D. V. Nanopoulos, and K. Tamvakis, *Phys. Lett.* **B121** (1983) 123; L. Alvarez-Gaume, J. Polchinski, and M. B. Wise, *Nucl. Phys.* **B221** (1983) 495.
- [17] K. Nakamura *et al.* [Particle Data Group], *J. Phys. G* **37**, 075021 (2010).
- [18] RAaij *et al.* [LHCb Collaboration], *Phys. Rev. Lett.* **110**, 021801 (2013).
- [19] Y. Amhis *et al.* [Heavy Flavor Averaging Group Collaboration], arXiv:1207.1158 [hep-ex].
- [20] D. Asner *et al.* [Heavy Flavor Averaging Group Collaboration], arXiv:1010.1589 [hep-ex].
- [21] G. Hinshaw *et al.* [WMAP Collaboration], arXiv:1212.5226 [astro-ph.CO].
- [22] H. Baer and M. Brhlik, *Phys. Rev. D* **55** (1997) 4463; H. Baer, M. Brhlik, D. Castano and X. Tata, *Phys. Rev. D* **58** (1998) 015007;
- [23] K. Babu and C. Kolda, *Phys. Rev. Lett.* **84** (2000) 228; A. Dedes, H. Dreiner and U. Nierste, *Phys. Rev. Lett.* **87** (2001) 251804; J. K. Mizukoshi, X. Tata and Y. Wang, *Phys. Rev. D* **66** (2002) 115003.
- [24] G. Aad *et al.* [ATLAS Collaboration], *Phys. Lett. B* **716**, 1 (2012) [arXiv:1207.7214 [hep-ex]].
- [25] S. Chatrchyan *et al.* [CMS Collaboration], *Phys. Lett. B* **716**, 30 (2012) [arXiv:1207.7235 [hep-ex]].
- [26] The ATLAS collaboration, ATLAS-CONF-2013-047.
- [27] G. Degrandi, S. Heinemeyer, W. Hollik, P. Slavich and G. Weiglein, *Eur. Phys. J. C* **28**, 133 (2003) [hep-ph/0212020]; T. Hahn, S. Heinemeyer, W. Hollik, H. Rzehak and G. Weiglein, *Phys. Rev. Lett.* **112**, 141801 (2014) [arXiv:1312.4937 [hep-ph]] and references therein.
- [28] I. Gogoladze, R. Khalid and Q. Shafi, *Phys. Rev. D* **80**, 095016 (2009) [arXiv:0908.0731 [hep-ph]].
- [29] S. Raza, Q. Shafi and C. S. Ün, arXiv:1412.7672 [hep-ph].
- [30] B. C. Allanach, S. Kraml and W. Porod, *JHEP* **0303**, 016 (2003) [hep-ph/0302102].